

Self-Assembled Hydrogel Fiber Bundles from Oppositely Charged Polyelectrolytes Mimic Micro-/Nanoscale Hierarchy of Collagen

Shilpa Sant,* Daniela F. Coutinho, Akhilesh K. Gaharwar, Nuno M. Neves, Rui L. Reis, Manuela E. Gomes, and Ali Khademhosseini*

Fiber bundles are present in many tissues throughout the body. In most cases, collagen subunits spontaneously self-assemble into a fibrillar structure that provides ductility to bone and constitutes the basis of muscle contraction. Translating these natural architectural features into a biomimetic scaffold still remains a great challenge. Here, a simple strategy is proposed to engineer biomimetic fiber bundles that replicate the self-assembly and hierarchy of natural collagen fibers. The electrostatic interaction of methacrylated gellan gum with a countercharged chitosan polymer leads to the complexation of the polyelectrolytes. When directed through a polydimethylsiloxane channel, the polyelectrolytes form a hierarchical fibrous hydrogel demonstrating nanoscale periodic light/dark bands similar to D-periodic bands in native collagen and align parallel fibrils at microscale. Importantly, collagen-mimicking hydrogel fibers exhibit robust mechanical properties (MPa scale) at a single fiber bundle level and enable encapsulation of cells inside the fibers under cell-friendly mild conditions. Presence of carboxyl- (in gellan gum) or amino- (in chitosan) functionalities further enables controlled peptide functionalization such as Arginylglycylaspartic acid (RGD) for biochemical mimicry (cell adhesion sites) of native collagen. This biomimetic-aligned fibrous hydrogel system can potentially be used as a scaffold for tissue engineering as well as a drug/gene delivery vehicle.

1. Introduction

In biological systems, fibrous structures self-assemble into a 3D hierarchical system at nano- to micro- and macroscale and are present in variety of tissues. In the heart,^[1] brain,^[2] bone,^[3] or skin,^[4] bundles of fibers, usually composed of collagen molecules as building blocks, are responsible for providing tensile strength to tissues. Collagen is the most abundant protein in the human body,^[5] thus receiving a great attention from the scientific community. Abnormalities in fiber formation or lack of collagen synthesis can lead to clinical scenarios where a serious reduction of tissue strength is observed. Osteogenesis imperfecta and arterial aneurysms are just two known examples of collagen-related diseases.^[6] Hodge and Petruska^[7] first proposed a 3D model for the structure of fibrillar collagen. Three left-handed helix polypeptide chains are twisted together

Dr. S. Sant,^[†] Dr. D. F. Coutinho, Dr. A. K. Gaharwar,^[††]

Prof. A. Khademhosseini
Center for Biomedical Engineering
Department of Medicine
Brigham and Women's Hospital
Harvard Medical School
Cambridge, MA 02139, USA
E-mail: shs149@pitt.edu; alik@bwh.harvard.edu

Dr. S. Sant, Dr. D. F. Coutinho, Dr. A. K. Gaharwar, Prof. A. Khademhosseini
Harvard-MIT Division of Health Sciences and Technology
Massachusetts Institute of Technology
Cambridge, MA 02139, USA

Dr. S. Sant, Dr. A. K. Gaharwar, Prof. A. Khademhosseini
Wyss Institute for Biologically Inspired Engineering
Harvard University
Boston, MA 02115, USA

Dr. D. F. Coutinho, Dr. N. M. Neves, Prof. R. L. Reis, Dr. M. E. Gomes
3B's Research Group – Biomaterials
Biodegradables and Biomimetics
Department of Polymer Engineering
University of Minho
Headquarters of the European Institute of Excellence on Tissue
Engineering and Regenerative Medicine
Ave Park, 4805-017 Barco, Guimarães, Portugal

DOI: 10.1002/adfm.201606273

Dr. D. F. Coutinho, Dr. N. M. Neves, Prof. R. L. Reis, Dr. M. E. Gomes
ICVS/3B's – PT Government Associate Laboratory
Braga/Guimarães, Portugal

^[†]Present address: Department of Pharmaceutical Sciences, School of Pharmacy, University of Pittsburgh, Pittsburgh, PA 15261, USA; Department of Bioengineering, Swanson School of Engineering, University of Pittsburgh, Pittsburgh, PA 15261, USA; McGowan Institute for Regenerative Medicine, University of Pittsburgh, Pittsburgh, PA 15261, USA

^[††]Present address: Department of Biomedical Engineering, Texas A&M University, College Station, TX 77841, USA; Department of Materials Science & Engineering, Texas A&M University, College Station, TX 77841, USA

 The ORCID identification number(s) for the author(s) of this article can be found under <https://doi.org/10.1002/adfm.201606273>.

into a right-handed coiled-coil triple helix, forming the collagen molecule, also known as tropocollagen. The internal hydrogen bonding between the nitrogen and carboxyl residues of the amino acids allows the stabilization of the tropocollagen structure, which is nearly 300 nm long. These tropocollagen molecules self-assemble linearly and laterally through electrostatic interactions, and the final structure is stabilized by hydrogen bonds and hydrophobic interactions. These structures result in collagen microfibrils (≈ 100 nm in diameter) with periodic striations, called *D*-bands ($D = 67$ nm)^[8] that result from preferential linear organization and a staggered orientation of the tropocollagen triple helix. Finally, these microfibrils assemble in parallel fiber bundles, forming fibers of ≈ 10 μ m in diameter (Figure S1A, Supporting Information).

Engineering materials that replicates the ability of collagen to form hierarchical assemblies with defined periodic and aligned features of collagen fibers in the body is therefore of great biomedical relevance. Numerous strategies for the development of synthetic fiber bundles have been proposed.^[9] Electrospinning has been widely reported for fiber formation.^[10] However, the high voltage required for its operation hampers its suitability for cell encapsulation. Extrusion of polymers from microfluidic channels into aqueous solutions is an alternative system for the production of fibers.^[9b,11] Although compatible for cell encapsulation, long incubation times for the material crosslinking, can decrease cell viability and functionality. While these technologies enable mimicry of the hierarchical organization at a microscale, they fail to achieve the most characteristic feature, axial *D*-periodicity of collagen fibers. A highly popular alternative is a bottom-up approach of self-assembly based on peptides,^[12] proteins,^[13] nucleic acids,^[14] or polysaccharides.^[15] Peptides have been the most explored building blocks for the formation of biomimetic fibrous systems.^[9c,d,12,16] For instance, Rele et al. have reported the synthesis of peptides capable of fibrillogenesis, forming striations with *D*-bands of ≈ 18 nm size,^[16a] which is considerably smaller than that reported for native collagen.^[8] These peptides were composed of positively and negatively charged amino acids and spontaneously self-assembled when incubated in buffer solution for 9 d. Despite their ability to mimic the native collagen structure at nanoscale, most of the peptide-based systems require fiber coarsening process to further thicken the formed fibers. This process is usually time consuming and requires an extra step in the process of engineering a synthetic fibrous system that requires external control. Moreover, the peptide fabrication itself is quite laborious and expensive. Another limitation of some of the existing engineered fiber bundles is that they may not be amenable for cell encapsulation inside the hydrogel systems, and the structural organization into multiple length scales within a cell-friendly, water-soluble system. In summary, self-assembled, aligned hydrogel fibers that replicate the nano- to microscale hierarchical structure including periodic *D*-bands of collagen fibers along with its biological properties to mediate the interactions between cells and the extracellular-matrix (ECM) is of extreme relevance and significance for biomedical applications.

A less studied approach is the self-assembly of polysaccharides into fibrous systems.^[15,17] Natural polysaccharides such as chitosan, alginate, hyaluronic acid, etc. offer enriched class of

materials with tunable physicochemical properties for development of drug/cell delivery to scaffolds for tissue engineering.^[18] Here, we present a self-assembled fibrous hydrogel prepared from two oppositely charged natural polysaccharides: cationic chitosan (CHT) and anionic gellan gum (GG). Gellan gum was methacrylated (MeGG) to offer additional stability to the fibrous structure by photocrosslinking.^[18a,f] A convenient microfluidic-based approach was used to direct the self-assembly and formation of the hydrogel fiber bundles. Furthermore, these individual fiber bundles showed nano- to microscale hierarchy, strong mechanical property, and biochemical mimicry of native collagen by providing Arginylglycylaspartic acid (RGD)-binding sites to the encapsulated human mesenchymal stem cells (hMSCs).

2. Results and Discussion

2.1. Microfluidic Channels Guide Self-Assembly of Oppositely Charged Polyelectrolytes into Aligned Hydrogel Fibers

To replicate the structural hierarchy of the collagen fibers, we took advantage of the electrostatic interaction that is known to occur between two charged polyelectrolytes. Many studies^[19] including ours^[18f] have reported polyelectrolyte complex formation between CHT and GG and studied effect of various process variables such as pH, charge density, etc. on polyelectrolyte complex properties. Specifically, in our own previous work,^[18f] we have tested three different ratios of chitosan and gellan gum (2:1, 1:1, and 1:2) and found fiber formation in the pores of these gels. Based on this observation, the objective of this work was to guide aligned fiber formation using microfluidic channels and study their hierarchical structure. We have explored different ratios of CHT and MeGG and found 1:1 ratio to be optimum in terms of efficient fiber formation without blocking the microfluidic channels or formation of excess gel (data not shown). Similarly, we have also explored higher concentrations of CHT and MeGG (2% w/v); however higher viscosities of these polymer solutions resulted in frequent blocking of the channels (data not shown). Hence, we selected 1% w/v solution as optimum concentration and 1:1 CHT:MeGG ratio for efficient fiber formation.

A fibrous hydrogel structure was fabricated by flowing aqueous solutions at 1% (w/v) of CHT and MeGG through two distinct channels engineered in polydimethylsiloxane (PDMS). The gelation of the polymers was triggered when one polymer came in contact with the other countercharged polymer, at the junction of the channels (Figure 1A). After polymer complexation, the common channel directed the polyelectrolyte complex (PEC) to the outlet of the PDMS channel, where hydrogel fiber was collected. CHT was used due to its proven potential for biomedical applications.^[18f,20] CHT is derived from chitin, the second most abundant natural polysaccharide, and it has been widely studied for the development of PECs.^[18f,21] CHT contains amine groups that were protonated at pH ≈ 4 of the solution used (1% v/v, acetic acid) (Figure S2, Supporting Information). Methacrylated GG (MeGG) has recently shown great potential in vivo for cartilage tissue engineering^[22] and can be easily synthesized by modification of the natural

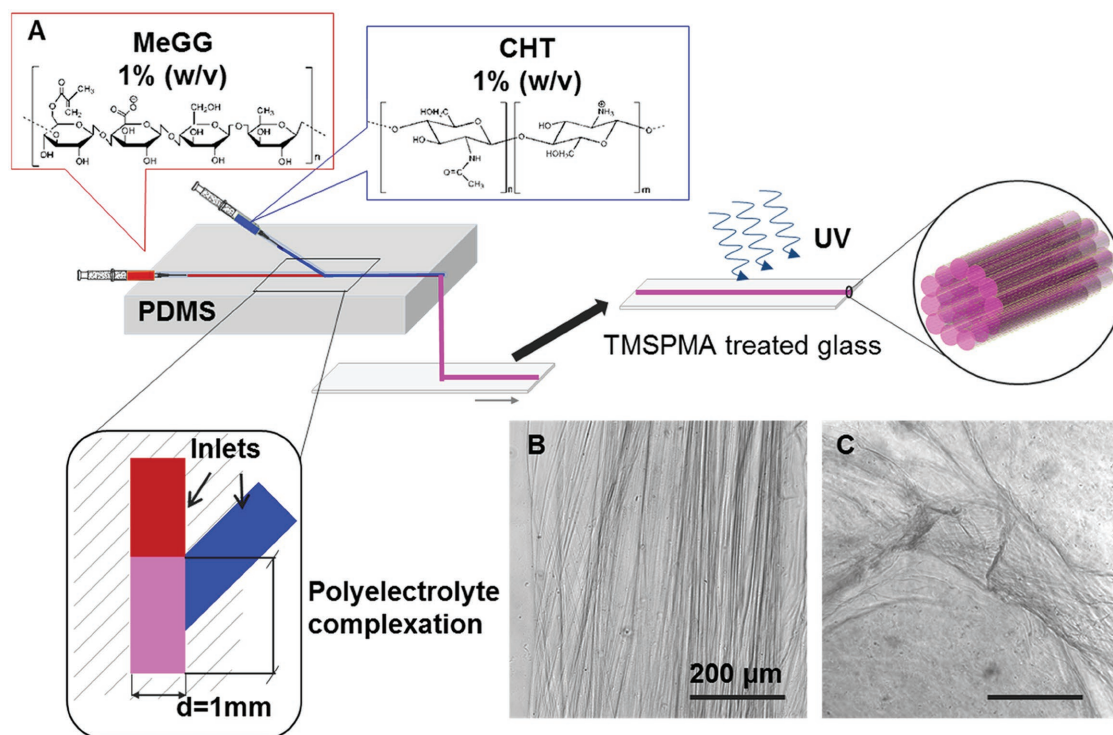


Figure 1. Fabrication of an aligned fibrous hydrogel. A) Schematics of fabrication of hydrogel fiber bundle with methacrylated gellan gum (MeGG) and chitosan (CHT). Both solutions are allowed to flow through separate channels within the PDMS mold. Complexation of the polyelectrolytes occurs in the channel where both solutions interact together. The hydrogel fiber bundle is collected onto a TMSPPMA treated glass slide and MeGG crosslinked with UV light. B) Optical microscopy of aligned engineered hydrogel fiber bundles and C) optical microscopy of nonaligned fibers, obtained by mixing both polymers randomly.

polymer, GG.^[18a] MeGG is a photocrosslinkable polymer and thus, can form hydrogels upon exposure to UV light. Both GG and MeGG can also be crosslinked by physical mechanisms (temperature and presence of ions) that induce formation of double helical segments followed by their aggregation and gel formation.^[23] This polymer was negatively charged under the conditions used in this study (Figure S2, Supporting Information). In a recent work, we have exploited the strong interaction between CHT and MeGG for PEC hydrogel formation.^[18f] It has been reported that PEC hydrogels may have poor hydrolytic stability since their crosslinking is dependent on the physicochemical properties of the environment.^[18f] Thus, in order to obtain a stable fibrous hydrogel, MeGG was photocrosslinked by UV exposure, stabilizing the hydrogel fibers. Given the small scale of these fibers (few hundred micrometers), they were collected onto siloxane treated glass slides. The presence of siloxane groups on the treated glass slide resulted in covalent binding of the methacrylated polymer to the glass slide, facilitating the handling and cell culture of these hydrogel fibers. The reported fluidic system enabled production of aligned fibrous structures, as observed in Figure 1B, in contrast with randomly formed fibers when both polymers were mixed randomly outside a channel (Figure 1C). Since the pH of both polymer solutions was different, we examined the possibility of the formation of the fibrous hydrogel due to the precipitation of one of the polymers as a result of pH change when mixed with the other polymer. To rule out this

possibility, MeGG was allowed to interact with an acetic acid solution (1% v/v) without CHT while in another experiment, CHT solution in acetic acid was allowed to interact with deionized water without MeGG. For both cases, where one of the polymers was replaced with only the solvent, no fibers were formed (data not shown). These results confirmed that formation of the fibers is uniquely the result of complexation of both polymers.

We next examined the distribution of both polymers within the fibrous hydrogel system. CHT was fluorescently labeled with fluorescein (Figure 2A). Distribution of CHT in the hydrogel fiber was evaluated by producing hydrogel fibers as described above using MeGG and fluorescein-CHT. Confocal microscopy of fluorescently labeled CHT in the *xyz* planes of the fiber bundle showed that CHT was present throughout the fibrous hydrogel (Figure 2B). Using the same fluorescently labeled system, we then evaluated the stability of the hydrogel fibers. Optical and fluorescent microscopy revealed that the fibers were stable and fluorescein-CHT was present even after 7 days of incubation of the hydrogel fibers in phosphate buffer saline (PBS) at 37 °C (Figure 2C). This showed that although only MeGG is covalently bonded to the treated glass slide, CHT was stable within the system for at least up to 7 days. These observations suggest that the electrostatic interactions between MeGG and CHT are strong enough, not only to form the fibrous hydrogel, but also to hold both polymers together.

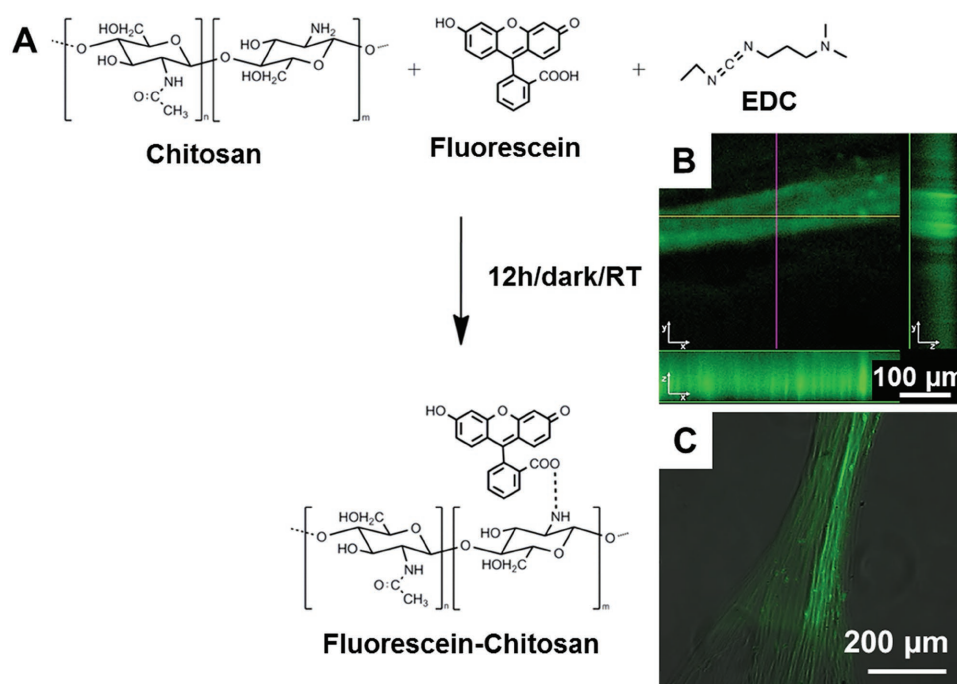


Figure 2. A) Synthesis scheme for fluorescein labeling of CHT (fluorescein-chitosan). B) Confocal image showing the distribution of fluorescein-CHT throughout the MeGG-CHT fiber bundle. C) The stability of fluorescein-CHT within MeGG-CHT fiber bundle after incubation for 7 days in PBS at 37 °C.

2.2. Self-Assembled Hydrogel Fibers Mimic Micro- to Nanoscale Hierarchy of Native Collagen

We further evaluated the microstructure of hydrogel fibers. The microscale structure of the fibrous hydrogel revealed organization into a fiber bundle, similar to that observed in natural collagen fibers. Scanning electron microscopy (SEM) of the top and side views of the system revealed that the fibrous hydrogel is constituted by several fibrils aligned in parallel and packed together in a bundle (Figure 3A,B). The morphology of the fibrous hydrogel was further confirmed by atomic force microscopy (AFM), indicating that the fibril size varied from 1 to 5 μm (Figure 3C,D and inset in D). Interestingly, we could observe a hierarchical organization of several fibrils assembled into a fiber closely resembling that of native collagen fibers. This structure, although architecturally similar to the natural one, is considerably bigger than that observed in human tissues.^[24] This was not surprising as the channels used were 1 mm in diameter; however, it can be tailored to form smaller fibers by modulating the channel diameter. Most importantly, these bundles also showed aligned fiber structure (Figure 3E) and birefringence (Figure 3F) when observed under polarized microscope.

Of note is the structure of fiber bundles observed at a nanoscale. Transmission electron microscopy (TEM) of a transverse cross-section of the fibrous hydrogel showed the presence of several circular structures packed together into a more complex structure (Figure 4A i–iii). These results suggested that a hierarchical organization of the engineered fibers observed at microscale is also present at sub-micrometer scale. The structural hierarchy resembling to that of the collagen fibers was

recapitulated by the presence of light and dark *D*-periodic bands, observed under TEM of the longitudinal section of the fibrous hydrogel (Figure 4B i–iii). The well-defined periodic light and dark bands were present perpendicular to the fiber length and across the entire width, orthogonal to the longitudinal fiber axis. Interestingly, the size of these periodic bands were about $D \approx 100\text{--}150$ nm, slightly higher than that reported for the native collagen fibers ($D = 67$ nm),^[8] whereas *D*-periodic bands reported when using self-assembling peptides were in the range of 18 nm.^[16a] In natural collagen, these features occur as a result of the staggered repetition of tropocollagen molecules, linearly self-assembled by electrostatic interactions, and laterally packed through hydrogen bonds and hydrophobic forces.^[16a,25] Similarly, the striations observed in hydrogel fiber bundles may correspond to the longitudinal repetition of oppositely charged CHT and MeGG polymer chains along the fiber main axis. This may be a result of the similar molecular configuration of both CHT and MeGG to the natural collagen molecules. For example, the proposed structure for hydrated CHT chains is a two-fold helix stabilized by intra- and intermolecular hydrogen bonds.^[26] On the other hand, plain GG molecular structure was proposed as a left-handed double helix, stabilized with three intrachain hydrogen bonds per tetrasaccharide unit, involving the D-glucuronate residues. The double helix is further stabilized by another three interchain hydrogen bonds in the interior of the GG molecule.^[27] Here, we propose a mechanism for the presence of striations orthogonal to the fiber axis. We hypothesize that the chains of MeGG and CHT self-assemble forming triple helices and are staggered linearly by electrostatic interactions occurring between the charged carboxylic groups of MeGG and the protonated amine of CHT

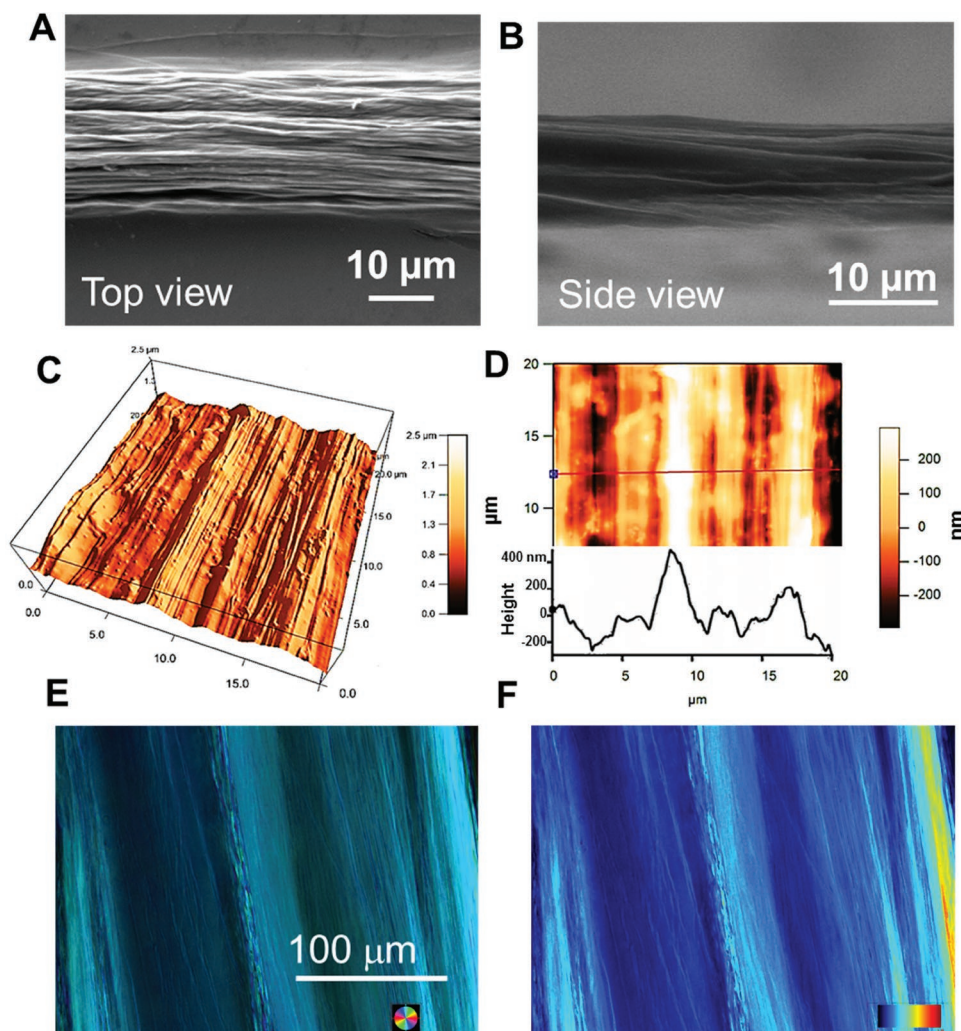


Figure 3. Microscale characterization of aligned hydrogel fiber bundle. Scanning electron microscopy of the A) top and B) side view of the hydrogel fiber bundle showing multiple microfibers aligned parallel to each other. C) 3D atomic force microscopy of the hydrogel fiber bundle. D) Height image of the hydrogel fiber bundles. Inset shows respective cross-section with fiber size 3–5 μm and height about 200–400 nm. E) Fiber alignment and F) birefringence probed by polarized microscopy. Inset in E and F shows the color key for alignment and birefringence, respectively.

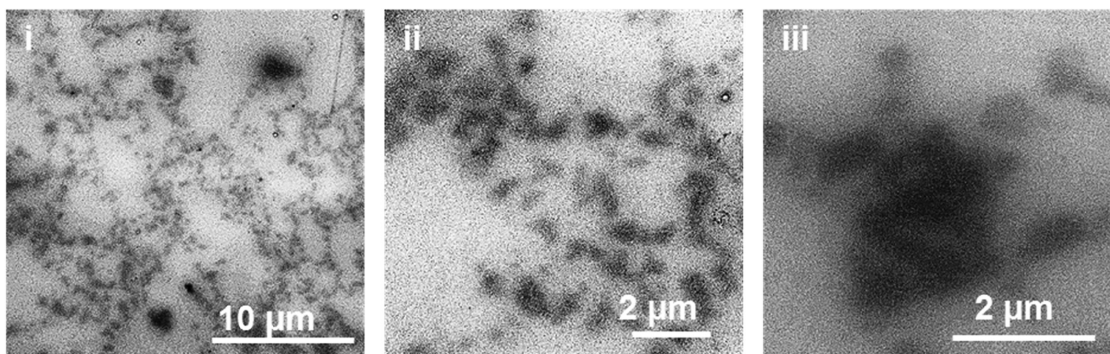
(Figure S1B, Supporting Information). The polymeric chains may further assemble laterally by hydrogen bonds. The stabilization of the fibrous hydrogel is further achieved by photocrosslinking MeGG and thus, covalently bonding parallel chains of MeGG. Although the above discussion is based on literature evidences of molecular configuration of CHT and GG molecules, our study does not provide definitive proof of molecular conformations adapted by these polymers when guided through the microfluidic channels. Thus, further studies such as X-ray scattering are required to get the diffraction pattern and support the above hypothesis about molecular conformations of CHT and MeGG in the hydrogel fiber structure. Nonetheless, to our knowledge, this is the first report of close biomimicry of nano- to microscale hierarchical organization (*D*-periodic bands to fibrils to fiber bundles) of native collagen using simple microfluidic assembly of oppositely charged polysaccharides over a time scale of seconds to minutes. Such mimicry of the hierarchical structure of native collagen fibers by directing the

self-assembly of two oppositely charged polysaccharides in a relative simple hydrogel system is of extreme importance for several biomedical and biotechnological applications.

2.3. Hierarchical Hydrogel Fiber Bundles Demonstrate Strong Mechanical Properties

We next asked if such hierarchical architecture mimicking native collagen fibers could also translate into some of the functional properties of collagen. As mentioned above, in many tissues in the body such as heart,^[1] brain,^[2] bone,^[3] and skin,^[4] collagen fibers are responsible for providing tensile strength to tissues. Hence, we characterized mechanical properties of self-assembled hydrogel fiber bundles. Despite their hydrogel nature, the uniaxial tensile tests performed in the direction parallel to the fiber axis revealed that these individual hydrogel fiber bundles (about 100 μm thick) are mechanically strong

A – Transversal Cross Section



B – Longitudinal Cross Section

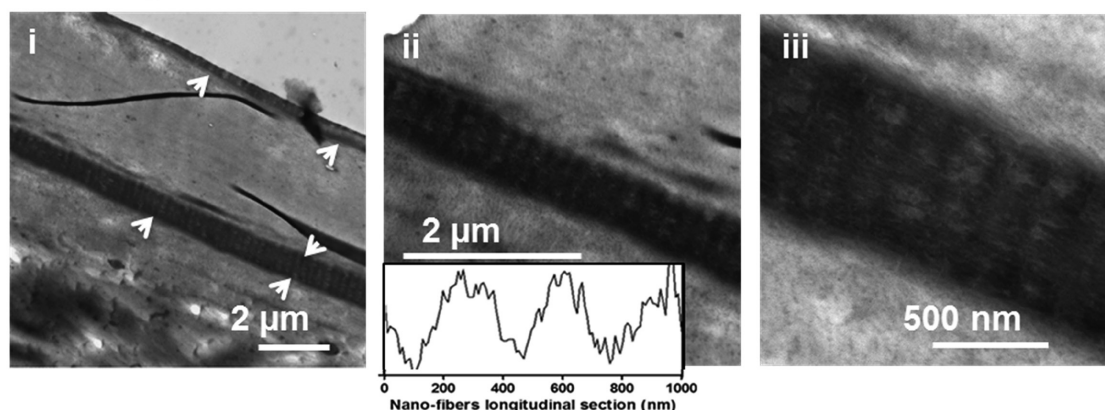


Figure 4. Characterization of the nanostructure of individual fibers. Transmission electron micrographs of A) transverse and B) longitudinal cross-sections of the hydrogel fibers bundles. Longitudinal section shows light and dark banding pattern (shown by arrowheads in B-i) perpendicular to the length of fibers. Inset in B-ii shows line graph of cross-section of banding pattern revealing the distance between two dark bands to be around 100–200 nm.

as evidenced by their elastic modulus of ≈ 3 MPa and tensile strength of ≈ 1 MPa (Figure 5A,B). This is important given that hydrogels generally have weak mechanical properties due to their high water content hampering their use for hard tissue engineering applications such as bone and teeth.^[18d,28] Due to thickness in the range of about 100 μm , we could not test the mechanical properties of single hydrogel fibers in the direction perpendicular to the fiber axis.

2.4. Biofunctionalization of MeGG with RGD Enables Biochemical Mimicry of Native Collagen

We further explored the effect of the aligned fibrils on directing the alignment of encapsulated fibroblasts and cardiomyocytes isolated from rat cardiac tissue (Figure S3, Supporting Information). After dissolving the MeGG polymer in cell culture media, cells were dispersed into the solution at physiological temperature, allowed to flow through the PDMS channel to form complex with CHT solution and finally, exposed briefly to UV light for the stabilization of the cell-encapsulating fibrous hydrogel onto the glass slide (Figure S3, Supporting Information). Encapsulated fibroblasts exhibited good viability (Figure S3Aii, Supporting Information) after fiber processing,

suggesting that the shear stress induced by the channel, the UV exposure and the slightly acidic pH of CHT solution did not have any major deleterious effects on the viability of fibroblasts. Confocal microscopy of these cells demonstrated that they are able to align along the fibril direction (Figure S3Aiii,iv, Supporting Information). Similarly, encapsulated cardiomyocytes revealed expression of cardiac markers, connexin and troponin, and alignment along the long fiber axis. However, these studies showed that although self-assembled polysaccharide fibrous hydrogels guided cellular alignment, they did not promote cell spreading. This may be due to lack of binding sites such as integrin in the polysaccharides. One of the functions of collagen in the body is providing integrin-binding sites for adhesion to the cells. Such biochemical mimicry to native collagen was achieved by covalently incorporating cell adhesive motifs (RGD) into the MeGG backbone (Figure 5C). Incorporation of RGD into MeGG backbone was confirmed by presence of nitrogen by X-ray photoelectron spectroscopy (XPS) (Figure 5D). After 7 days in culture, hMSCs seeded on the glass cover slips (2D-glass) were able to attach and spread randomly. Similarly, cells seeded on top of unprocessed MeGG-RGD hydrogels (not fibers) were able to attach and spread within 12–48 h (Figure 5E). We then fabricated hydrogel fiber bundles using either MeGG as described earlier or RGD-functionalized

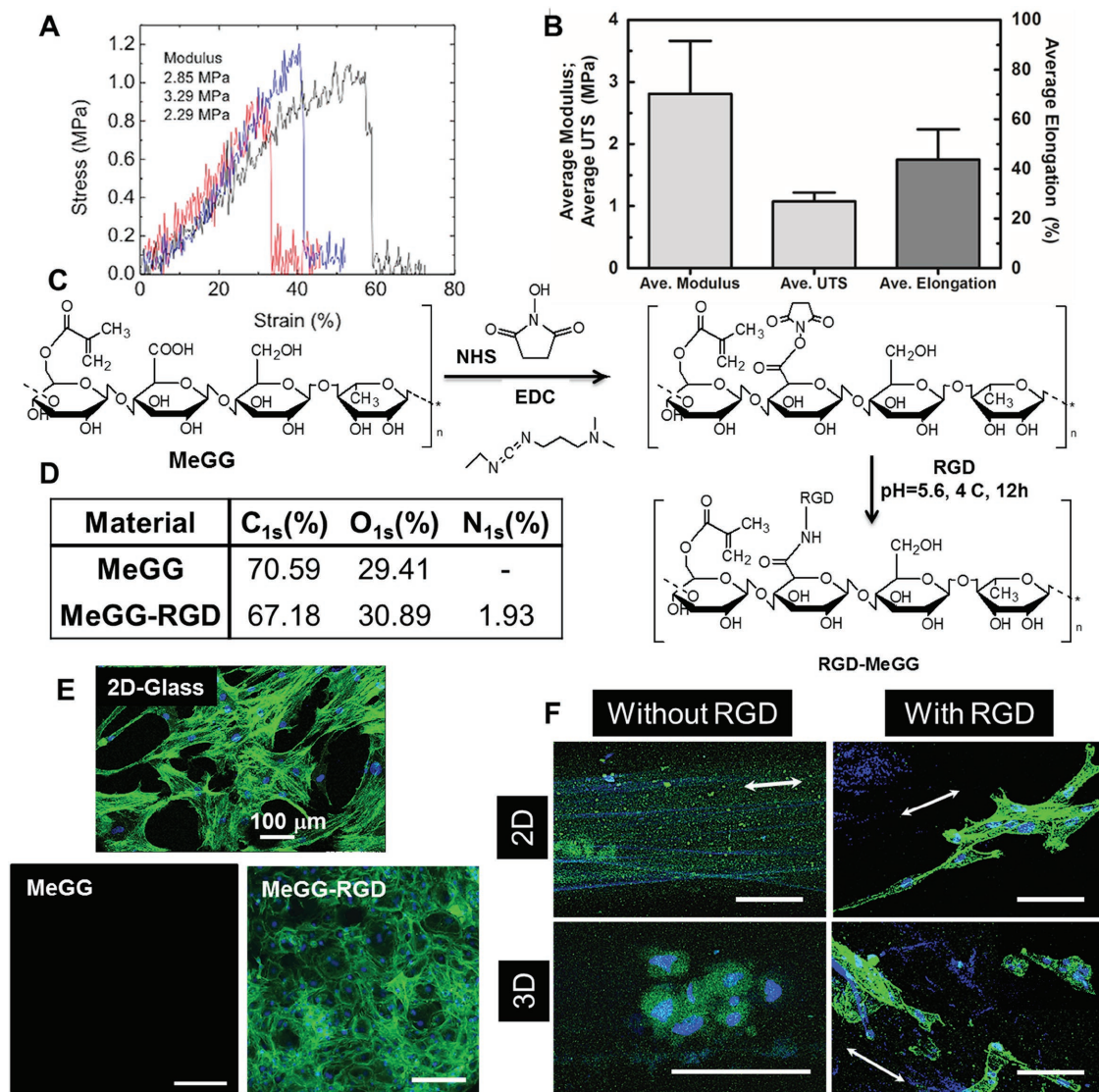


Figure 5. Mechanical properties of hierarchical fiber bundles and biochemical mimicking of collagen. A) Representative stress–strain curves of three individual hydrogel fiber bundles with B) average modulus of about 3 MPa and tensile strength (UTS) of 1 MPa. C) Synthesis scheme of RGD-functionalized MeGG to mimic integrin binding sites present in the native collagen. D) Elemental analysis of modified MeGG-RGD by XPS revealed presence of nitrogen in MeGG-RGD. E) Human MSCs seeded on 2D glass cover slips show spread morphology. MeGG gels alone do not support cell attachment while RGD biofunctionalization (MeGG-RGD) supports cell attachment and spreading on top of these gels; Scale bar: 100 μm. F) Only RGD biofunctionalization provides integrin binding sites allowing attachment and spreading of hMSCs on the fiber bundle (2D) and when encapsulated inside the bundle (3D). Fiber bundles prepared from MeGG without RGD show minimum cell attachment in 2D and rounded cell morphology of hMSCs encapsulated inside the bundles in 3D. Double-headed arrows indicate fiber direction. Scale bars: 100 μm.

MeGG (MeGG-RGD). We seeded hMSCs either on top of the fiber bundle (2D culture) or encapsulated hMSCs inside the fiber bundles (3D encapsulation) as described for fibroblasts/cardiomyocytes. Fibers of CHT-MeGG without RGD did not show good cell attachment while CHT-MeGG-RGD fibers were able to attach and importantly, spread along the direction of fiber axis (Figure 5F, 2D, green: actin-phalloidin). When encapsulated, the CHT-MeGG hydrogel fibers were able to retain hMSCs inside the fibers; however, they did not support spreading of these cells as evidenced by rounded morphology. On the other hand, hMSCs encapsulated inside CHT-MeGG-RGD fibers showed spreading along the fiber axis (Figure 5F,

3D, bottom panel). Presence of carboxylic groups on GG and amino groups on CHT enables biofunctionalization using any biomolecule such as RGD, fibronectin, laminin, etc. in the fibrils to improve the extracellular matrix microenvironment for a specific application.

3. Conclusion

We have reported fabrication of a biomimetic fibrous hydrogel that replicates the hierarchical structure of natural collagen fibers from nano- to microscale (axial *D*-periodicity to

microfibrils to fiber bundle). A simple method that combines the properties of oppositely charged polyelectrolytes and the ability of a fluidic channel to direct the flow of a solution was employed. A fibrous hydrogel was engineered by flowing the anionic MeGG and the cationic CHT through two PDMS channels. At the channel junction, polymer chains of MeGG interacted with those of CHT forming PEC fibers. At micrometer scale, the engineered structure was organized into a bundle of microfibrils. The natural nanoscale features of collagen fibers were also replicated into the engineered fibrous hydrogel by the presence of periodic *D*-bands ($D \approx 100$ nm). We have proposed a mechanism for the formation of these striations. We hypothesize that similar to the mechanism occurring in natural fibers, polymeric chains of MeGG and CHT self-assemble linearly and laterally by electrostatic interactions and are stabilized by hydrogen bonds. Furthermore, these aligned hydrogel fibers enabled encapsulation of many different cell types such as rat cardiac fibroblasts, cardiomyocytes, and hMSCs in cell-friendly mild conditions without affecting their viability. Biofunctionalization with RGD provided cell adhesion sites for attachment and spreading of hMSCs demonstrating biochemical mimicry of native collagen integrin binding sites. We emphasize that the unique property of using the photocrosslinkable MeGG allows the possibility to tune the physicochemical and mechanical properties of these hydrogel fibers for broader application in tissue engineering. The developed aligned hydrogel fibers are potentially useful for a variety of systems, from neural tissue, skeletal muscle, cardiac muscle to bone.

4. Experimental Section

Materials and Solutions: CHT was purchased from Sigma-Aldrich (USA) and MeGG was synthesized as described earlier.^[18a] Briefly, gellan gum (1% w/v, GG, Gelrite, Sigma-Aldrich, USA) was dissolved in deionized water at 90 °C for 20–30 min. Methacrylic anhydride (8% v/v) was added at 50 °C and the reaction continued for 6 h at pH 8.0. The modified MeGG polymer was dialyzed (Fisher Scientific, membrane with molecular weight cutoff of 11–14 kDa, USA), freeze-dried, and stored at a dry place protected from light until further use. CHT and MeGG were dissolved (1% v/v), respectively, in an aqueous solution of acetic acid and in deionized water under constant stirring at 50 °C for 10 min. Photoinitiator 2-hydroxy-1-[4-(2-hydroxyethoxy)phenyl]-2-methyl-1-propanone (Irgacure 2959, Ciba Specialty Chemicals) was added (0.5% w/v) to MeGG for chemical crosslinking. All other reagents were purchased from Sigma-Aldrich unless specifically mentioned.

Hydrogel Fiber Bundle Fabrication: Aligned hydrogel fibers were fabricated by combining polyelectrolyte complexation and microfluidics technology. Briefly, a fluidic device (Figure 1) with two oblique channels (1 mm diameter) was fabricated using PDMS and template-based technology. MeGG solution (1% w/v, with or without cells) and CHT (1% w/v) solution were injected in each inlet of the microfluidic device and the flow was maintained with a syringe pump (50 mL h^{-1}). At the position where the two solutions merged, the oppositely charged chains of MeGG and CHT interacted through the electrostatic forces. The formed fibers were collected onto 3-(trimethoxysilyl) propyl methacrylated (TMSPMA) treated glass slides. The collected fibers were stabilized by exposure to light ($320\text{--}500 \text{ nm}$, 1.2 mW cm^{-2} , EXFO OmniCure S2000) for 60 s.

Hydrogel Fiber Bundle Characterization: Distribution of CHT within the Hydrogel Fiber Bundle: Fluorescein-labeled CHT was used in the development of the hydrogel fiber bundle in order to evaluate the

distribution of CHT within the hydrogel structure. Fluorescein-CHT conjugate was synthesized as described elsewhere.^[31] Briefly, the amine groups of CHT were reacted with the carboxylic groups of fluorescein, forming amide bonds (Figure 2A). The pH of the solution was adjusted to 8 with 5.0 M NaOH. Fluorescein, previously dissolved in ethanol (0.1% w/v), was added to the CHT solution (4% v/v). 1-ethyl-3-(3-dimethylaminopropyl) carbodiimide hydrochloride (0.05 M, EDC, Thermo Scientific) was added to catalyze the formation of amide bonds. The reaction continued for 12 h under permanent stirring in the dark and at room temperature (RT). The fluorescein-CHT conjugate was purified by dialysis (Fisher Scientific, membrane with molecular weight cutoff of 11–14 kDa, USA) for at least 3 days against distilled water to remove the unreacted fluorescein. Purified CHT was obtained by lyophilization and stored at a dry place protected from light until further use.

The hydrogel fiber bundles prepared with fluorescein-CHT were kept in phosphate buffered saline (PBS, Gibco) at 37 °C for 7 days in order to evaluate the stability of CHT within the hydrogel structure. The distribution of fluorescein-CHT in MeGG hydrogel fiber bundle was probed by imaging in the *xyz* direction (*z*-stack) using confocal laser scanning microscope (Olympus FV300, Melville, NY) and fluorescence was detected upon excitation at 488 nm through a cutoff dichroic mirror and an emission band-pass filter of 505–530 nm. Freshly prepared hydrogel fibers of plain (nonfluorescent) CHT-MeGG were also imaged under polarized microscope equipped with Abrio camera (CRI, Inc.) to investigate if they show any birefringence.

Scanning Electron Microscopy (SEM): The microscale morphology of the hydrogel fiber bundles was further observed using a scanning electron microscope (Zeiss Ultra 55, Germany). Hydrogels were flash-frozen in liquid nitrogen and freeze-dried for 72 h, as previously described.^[17b] Samples were sputter-coated (SP-2 AJA Sputtering System) with a palladium–platinum alloy with 40 mA current for 80 s before SEM observation. The images were captured at 15 kV.

Atomic Force Microscopy: AFM images were acquired by a Multimode Nanoscope V (Veeco) in order to examine the micro-/nanoscale morphology of the hydrogel fibers. A commercial cantilever probe, with a thickness of 4 μm and a tip radius of 10–12.5 nm was used. The probe oscillation resonance frequency was ≈ 100 kHz. All the samples were characterized using a set-point amplitude ratio of ≈ 0.7 . Images were captured at room temperature, at different locations and with an area of 25 μm^2 . Images were processed and analyzed by multimode software Nanoscope V6.13.

Transmission Electron Microscopy: The internal nanostructure of the hydrogel fiber bundles was analyzed by embedding freshly prepared samples and analyzing the transverse and longitudinal cross-sections of the hydrogel structure. The samples were prepared by fixing hydrated hydrogels in 2% glutaraldehyde/2% paraformaldehyde and treated with 1% osmium tetroxide for 1 h at RT. The samples were then dehydrated in 70%, 95%, 2 \times 100% ethanol and then embedded in Epon resin, polymerized at 60 °C for 48 h. Ultrathin 70–80 nm thick sections were cut and mounted on the formvar/carbon-coated grids and observed under TEM (Tecnaï G² Spirit BioTWIN, FEI).

Mechanical Characterization: Mechanical properties of freshly prepared individual hydrogel fibers ($n = 5$) were investigated by uniaxial mechanical testing (Instron 5542 mechanical tester) as described before^[32] with slight modifications. Just before the testing, images of the fibers were captured to accurately measure the diameter of each fiber to calculate the cross-sectional area (NIH Image). The fibers were stretched until failure at a constant strain rate of 10 mm min^{-1} . The stress (MPa) was obtained by dividing the applied force (*N*) with cross-section area and percentage elongation (strain) was obtained from the displacement using $((L - L_0)/L_0/100)$, where L_0 was initial gauge length (1.5 mm) and *L* was instantaneous gauge length. Ultimate tensile strength (UTS) was recorded as the maximum stress at sample failure. Elastic modulus was calculated from the linear part of the stress–strain curve.

Viability Studies on Encapsulated Rat Cardiac Fibroblasts and Cardiomyocytes: Rat cardiac fibroblasts were isolated from the heart of

a 1 day-old Sprague-Dawley rat.^[31] Briefly, hearts ($n = 10$) were washed with Hank's balanced salt solution (HBSS, Gibco Invitrogen Co., USA) in order to remove the excess of blood. Tissues were minced and incubated in a solution containing collagenase (0.3 mg mL^{-1}) and pancreatin (0.6 mg mL^{-1}) (Sigma Chemical Co., USA). Isolated cells were preincubated for 30 min in Dulbecco's modified Eagles' medium (DMEM, Gibco Invitrogen), supplemented with 10% of heat-inactivated fetal bovine serum (FBS, Sigma) and 1% penicillin–streptomycin (Gibco Invitrogen), at 37°C and 5% CO_2 . Rat cardiac fibroblast population was purified by changing the medium and separating the nonadherent cardiomyocyte cells. Once confluence was reached, rat cardiac fibroblasts were trypsinized (trypsin/EDTA solution, Gibco) and suspended ($17 \text{ million cells mL}^{-1}$) in the MeGG solution, previously warmed to 37°C . Fibrous hydrogels were prepared as described before, using plain CHT and MeGG with suspended rat cardiac fibroblasts. After stabilization with UV exposure, fibrous hydrogels were cultured for up to 7 days in 6-well-plates (Fisher Scientific) under standard culture conditions, with media exchanged every 48 h. Viability of cells encapsulated after 7 days of culture was evaluated by incubating cells with a Live/Dead (Invitrogen) assay (calcein AM/ethidium homodimer-1 in Dulbecco's phosphate buffered saline, DPBS) for 20 min. Cell alignment was assessed by immunostaining of the cell cytoskeleton with phalloidin and counterstaining their nuclei with DAPI (4',6-diamidino-2-phenylindole). Similarly, cardiomyocytes were suspended in MeGG solution immediately after isolation and encapsulated in the hydrogel fibers as described above. After 7 days of culture, the cells were stained with cardiomyocyte markers, troponin, and connexin 43 (Abcam) as described before.^[32]

Biochemical Mimicry: RGD Functionalization of the Hydrogel Fiber Bundle to Mimic Integrin Binding Sites Present in Native Collagen: RGD sequence was covalently bound to MeGG using carbodiimide chemistry. Briefly, MeGG (100 mg) was dissolved in 2-(N-morpholino) ethanesulfonic acid (MES) buffer, pH 6.0 at around 50°C . To this solution, EDC (88 mg, Sigma) and N-Hydroxysuccinimide (NHS, 0.2 g, Sigma) were added and allowed to react for 2 h at 37°C . Then, RGD ($35 \mu\text{L}$, 1 mg mL^{-1} , Sigma) was added and the reaction was continued overnight at RT. The solution was dialyzed for 2 days and kept at 4°C after freeze-drying. RGD functionalization was confirmed by elemental analysis by X-ray photoelectron spectroscopy (XPS).^[18f] The analysis was performed on a Kratos Axis Ultra XPS instrument using a monochromatic Al $K\alpha$ X-ray source operating at 15 kV and 10 mA. The elements in the sample surface were identified from a survey spectrum at pass energy of 160 eV. The areas under the specific peaks were used to calculate the atomic percentages.

RGD functionalization was further confirmed by cell attachment studies. 2D hydrogels were fabricated by UV exposure and cardiac fibroblasts ($2 \times 10^6 \text{ cells mL}^{-1}$) were seeded on top of 2D MeGG or MeGG-RGD hydrogel (unprocessed isotropic MeGG hydrogels). These cells were stained with cytoskeletal actin phalloidin and imaged for cell attachment and spreading to further confirm successful RGD functionalization of MeGG.

To further investigate if CHT-MeGG-RGD is capable of promoting cell encapsulation and cell spreading, CHT-MeGG hydrogel fibers were fabricated by using CHT and either MeGG or RGD-functionalized MeGG (MeGG-RGD) to mimic integrin-binding sites in the native collagen. hMSCs were cultured as described earlier.^[33] Briefly, bone marrow-derived human mesenchymal stem cells (PT-2501, Lonza) were grown in normal growth media (Poietics MSCGM BulletKit, PT-3001, Lonza). The cells were cultured until 70–75% confluence and were used before passage 5 for all the experiments. The hMSCs were seeded either on top of the fibers (2D, $1 \times 10^6 \text{ mL}^{-1}$) or encapsulated inside the fibers (3D, $2 \times 10^6 \text{ mL}^{-1}$). The hMSCs seeded in 2D glass were used as control. After 7 days in culture, the cells-seeded fibers were fixed with 4% paraformaldehyde for 30 min, permeabilized with 0.1% triton X-100 in PBS containing 1% bovine serum albumin (BSA) and stained for alexa-fluor 488-labeled actin-phalloidin (Abcam) and visualized by confocal laser scanning microscope (Leica).

Supporting Information

Supporting Information is available from the Wiley Online Library or from the author.

Acknowledgements

S.S. and D.F.C. contributed equally to the work. This research was funded by the US Army Engineer Research and Development Center, the Institute for Soldier Nanotechnology, the NIH (HL092836, EB007249), and the National Science Foundation CAREER award (A.K.). This work was in part supported by FCT through funds from the POCTI and/or FEDER programs and from the European Union under the project NoE EXPERTISSUES (NMP3-CT-2004-500283). D.F.C. acknowledges the Foundation for Science and Technology (FCT), Portugal and the MIT-Portugal Program for personal grant SFRH/BD/37156/2007. S.S. acknowledges the postdoctoral fellowship awarded by Le Fonds Quebecois de la Recherche sur la Nature et les Technologies (FQRNT), Quebec, Canada and interdisciplinary training fellowship (NIH NRSA T32) awarded by System-based Consortium for Organ Design and Engineering (SysCODE). The authors would like to thank Dr. Iva Pashkuleva and Dr. Maria Ericsson for scientific discussions and technical assistance with TEM, respectively.

Keywords

bottom-up self-assembly, chitosan and gellan gum, collagen mimicking, hierarchical hydrogel fibers, polyelectrolyte complexes

Received: November 28, 2016

Published online:

- [1] D.-H. Kim, E. A. Lipke, P. Kim, R. Cheong, S. Thompson, M. Delannoy, K.-Y. Suh, L. Tung, A. Levchenko, *Proc. Natl. Acad. Sci. USA* **2010**, *107*, 565.
- [2] H. M. Finlay, L. McCullough, P. B. Canham, *J. Vasc. Res.* **1995**, *32*, 301.
- [3] S. Weiner, H. D. Wagner, *Annu. Rev. Mater. Sci.* **1998**, *28*, 271.
- [4] C. Prost-Squarcioni, S. Fraitag, M. Heller, N. Boehm, *Ann. Dermatol. Venereol.* **2008**, *135*, S5.
- [5] K. Gelse, E. Poschl, T. Aigner, *Adv. Drug Delivery Rev.* **2003**, *55*, 1531.
- [6] J. Myllyharju, K. I. Kivirikko, *Ann. Med.* **2001**, *33*, 7.
- [7] A. Hodge, J. Petruska, in *Aspects of Protein Structure* (Ed: G. Ramachandran), Academic, London **1963**, p. 289.
- [8] M. D. Shoulders, R. T. Raines, *Annu. Rev. Biochem.* **2009**, *78*, 929.
- [9] a) A. Martins, M. L. A. da Silva, S. Faria, A. P. Marques, R. L. Reis, N. M. Neves, *Macromol. Biosci.* **2011**, *11*, 978; b) C. M. Hwang, A. Khademhosseini, Y. Park, K. Sun, S.-H. Lee, *Langmuir* **2008**, *24*, 6845; c) D. E. Przybyla, J. Chmielewski, *Biochemistry* **2010**, *49*, 4411; d) S. M. Zhang, M. A. Greenfield, A. Mata, L. C. Palmer, R. Bitton, J. R. Mantei, C. Aparicio, M. O. de la Cruz, S. I. Stupp, *Nat. Mater.* **2010**, *9*, 594.
- [10] a) Z. Tong, S. Sant, A. Khademhosseini, X. Jia, *Tissue Eng., Part A* **2011**, *17*, 2773; b) S. Sant, A. Khademhosseini, *Conf. Proc. IEEE Eng. Med. Biol. Soc.* **2010**, *1*, 3546; c) S. Sant, C. M. Hwang, S.-H. Lee, A. Khademhosseini, *J. Tissue Eng. Regen. Med.* **2011**, *5*, 283; d) S. Soliman, S. Sant, J. W. Nichol, M. Khabry, E. Traversa, A. Khademhosseini, *J. Biomed. Mater. Res., Part A* **2011**, *96A*, 566; e) S. Mukundan, V. Sant, S. Goenka, J. Franks, L. C. Rohan, S. Sant, *Eur. Polym. J.* **2015**, *68*, 21.

- [11] a) C. M. Hwang, Y. Park, J. Y. Park, K. Lee, K. Sun, A. Khademhosseini, S. H. Lee, *Biomed. Microdevices* **2009**, *11*, 739; b) M. Hu, R. Deng, K. M. Schumacher, M. Kurisawa, H. Ye, K. Purnamawati, J. Y. Ying, *Biomaterials* **2010**, *31*, 863.
- [12] D. Papapostolou, A. M. Smith, E. D. T. Atkins, S. J. Oliver, M. G. Ryadnov, L. C. Serpell, D. N. Woolfson, *Proc. Natl. Acad. Sci. USA* **2007**, *104*, 10853.
- [13] T. O. Yeates, J. E. Padilla, *Curr. Opin. Struct. Biol.* **2002**, *12*, 464.
- [14] N. C. Seeman, *Biochemistry* **2003**, *42*, 7259.
- [15] A. C. A. Wan, I. C. Liao, E. K. F. Yim, K. W. Leong, *Macromolecules* **2004**, *37*, 7019.
- [16] a) S. Rele, Y. Song, R. P. Apkarian, Z. Qu, V. P. Conticello, E. L. Chaikof, *J. Am. Chem. Soc.* **2007**, *129*, 14780; b) D. N. Woolfson, M. G. Ryadnov, *Curr. Opin. Chem. Biol.* **2006**, *10*, 559.
- [17] B. C. U. Tai, A. C. A. Wan, J. Y. Ying, *Biomaterials* **2010**, *31*, 5927.
- [18] a) D. F. Coutinho, S. V. Sant, H. Shin, J. T. Oliveira, M. E. Gomes, N. M. Neves, A. Khademhosseini, R. L. Reis, *Biomaterials* **2010**, *31*, 7494; b) C. M. Hwang, S. Sant, M. Masaeli, N. N. Kachouie, B. Zamanian, S. H. Lee, A. Khademhosseini, *Biofabrication* **2010**, *2*, DOI:10.1088/1758-5082/2/3/035003; c) J. Rabanel, N. Bertrand, S. Sant, S. Louati, P. Hildgen, in *Polysaccharides for Drug Delivery and Pharmaceutical Applications*, Vol. 934 (Eds: R. H. Marchessault, F. Ravenelle, X. Zhu), American Chemical Society, Washington **2006**, p. 305; d) S. Sant, M. J. Hancock, J. P. Donnelly, D. Iyer, A. Khademhosseini, *Can. J. Chem. Eng.* **2010**, *88*, 899; e) S. Yamanlar, S. Sant, T. Boudou, C. Picart, A. Khademhosseini, *Biomaterials* **2011**, *32*, 5590; f) D. F. Coutinho, S. Sant, M. Shakiba, B. Wang, M. E. Gomes, N. M. Neves, R. L. Reis, A. Khademhosseini, *J. Mater. Chem.* **2012**, *22*, 17262.
- [19] a) K. A. M. Amin, M. in het Panhuis, *Carbohydr. Polym.* **2011**, *86*, 352; b) C. S. Picone, R. L. Cunha, *Carbohydr. Polym.* **2013**, *94*, 695; c) A. J. Granero, J. M. Razal, G. G. Wallace, M. in het Panhuis, *Macromol. Biosci.* **2009**, *9*, 354; d) L. Liu, B. Wang, Y. Gao, T. C. Bai, *Carbohydr. Polym.* **2013**, *97*, 152.
- [20] a) J. Berger, M. Reist, J. M. Mayer, O. Felt, N. A. Peppas, R. Gurny, *Eur. J. Pharm. Biopharm.* **2004**, *57*, 19; b) N. Bhattarai, J. Gunn, M. Q. Zhang, *Adv. Drug Delivery Rev.* **2010**, *62*, 83.
- [21] a) A. V. Ili'ina, V. P. Varlamov, *Appl. Biochem. Microbiol.* **2005**, *41*, 5; b) G. Lawrie, I. Keen, B. Drew, A. Chandler-Temple, L. Rintoul, P. Fredericks, L. Grondahl, *Biomacromolecules* **2007**, *8*, 2533; c) C. Deng, P. C. Zhang, B. Vulesevic, D. Kuraitis, F. F. Li, A. F. Yang, M. Griffith, M. Ruel, E. J. Suuronen, *Tissue Eng., Part A* **2010**, *16*, 3099.
- [22] J. T. Oliveira, T. C. Santos, L. Martins, R. Picciochi, A. P. Marques, A. G. Castro, N. M. Neves, J. F. Mano, R. L. Reis, *Tissue Eng. Part A* **2009**, *16*, 343.
- [23] H. Grasdalen, O. Smidsrod, *Carbohydr. Polym.* **1987**, *7*, 371.
- [24] M. Buehler, *Current Appl. Phys.* **2008**, *8*, 440.
- [25] a) J. A. Fallas, L. E. R. O'Leary, J. D. Hartgerink, *Chem. Soc. Rev.* **2010**, *39*, 3510; b) S. M. Yu, Y. Li, D. Kim, *Soft Matter* **2011**, *7*, 7927.
- [26] E. Franca, R. Lins, L. Freitas, T. Straatsma, *J. Chem. Theory Comput* **2008**, *4*, 2141.
- [27] R. Chandrasekaran, R. Millane, S. Arnott, E. Atkins, *Carbohydrate Research* **1988**, *175*, 1.
- [28] a) S. Sant, D. F. Coutinho, N. Sadr, R. L. Reis, A. Khademhosseini, *Biomimetic Approaches for Biomaterials Development*, Wiley-VCH Verlag GmbH & Co. KGaA, **2012**, pp. 471–493; b) M. K. Jaiswal, J. R. Xavier, J. K. Carrow, P. Desai, D. Alge, A. K. Gaharwar, *ACS Nano* **2016**, *10*, 246.
- [29] A. M. de Campos, Y. Diebold, E. L. S. Carvalho, A. Sanchez, M. J. Alonso, *Pharm. Res.* **2004**, *21*, 803.
- [30] a) A. K. Gaharwar, M. Nikkah, S. Sant, A. Khademhosseini, *Biofabrication* **2015**, *7*, 015001; b) Y. Xue, A. Patel, V. Sant, S. Sant, *Eur. Polym. J.* **2015**, *72*, 163.
- [31] A. Khademhosseini, G. Eng, J. Yeh, P. A. Kucharczyk, R. Langer, G. Vunjak-Novakovic, M. Radisic, *Biomed. Microdevices* **2007**, *9*, 149.
- [32] Y.-S. Hwang, B. G. Chung, D. Ortmann, N. Hattori, H.-C. Moeller, A. Khademhosseini, *Proc. Natl. Acad. Sci. USA* **2009**, *106*, 16978.
- [33] A. K. Gaharwar, S. M. Mihaila, A. Swami, A. Patel, S. Sant, R. L. Reis, A. P. Marques, M. E. Gomes, A. Khademhosseini, *Adv. Mater.* **2013**, *25*, 3329.